Soy Protein Adhesives with Water and Heat Resistant, and Magnetic Properties *via* Micron/Nanometer Iron-based Particle Modification

Jiawen Cao, Chen Chen, and Wei Xu *

* *Corresponding author: xuwei@njfu.edu.cn*

DOI: 10.15376/biores.21.1.873-889

GRAPHICAL ABSTRACT

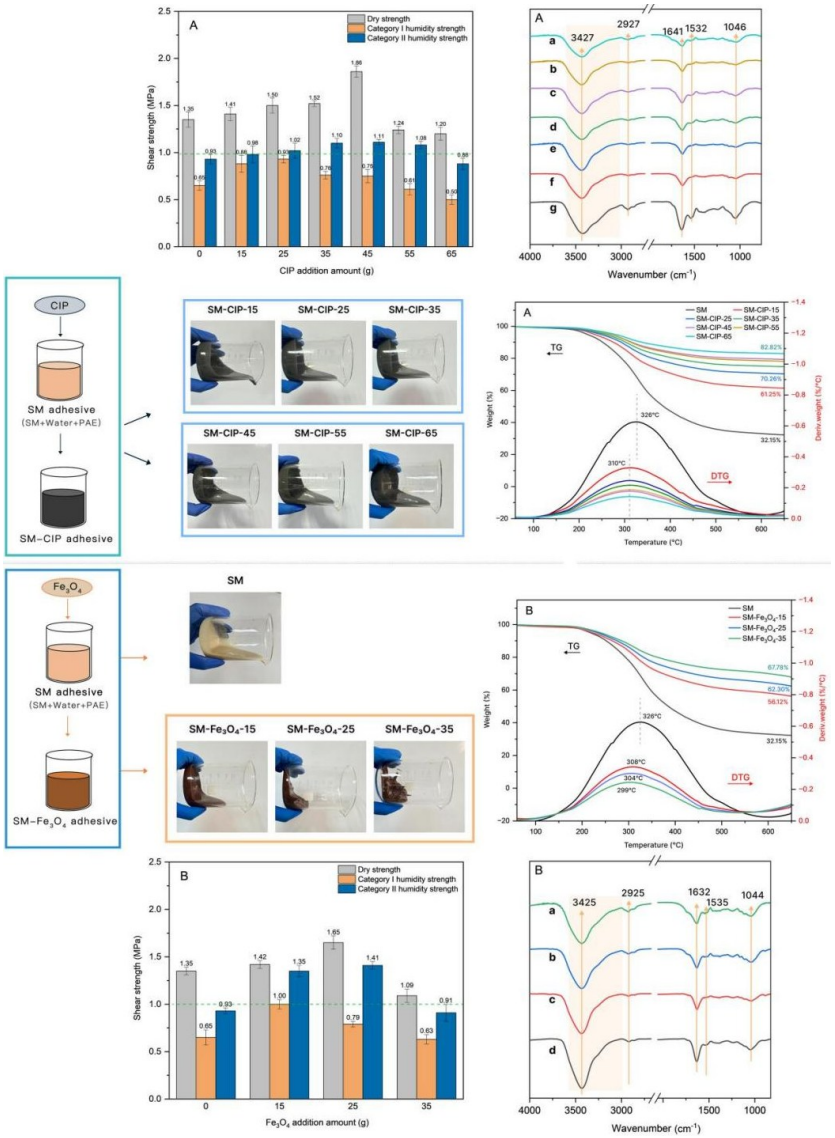

Soy Protein Adhesives with Water and Heat Resistant, and Magnetic Properties *via* Micron/Nanometer Iron-based Particle Modification

Jiawen Cao, Chen Chen, and Wei Xu *

The development of soybean meal (SM)-based adhesives with water resistance, heat tolerance, and magnetic-adsorbent functions is critical for expanding their applications as wood adhesives in hot and humid kitchen environments. A key goal is to enable magnetic storage systems such as knife holders and detachable shelves through localized adhesive application. However, the monofunctionality of existing bio-based adhesives limits their practical potential. In this study, micron-sized carbonyl iron powder (CIP) and nanoscale ferrosoferric oxide (Fe_3O_4) were introduced to confer multifunctionality to SM adhesives. Results indicated that the micron-scale dispersion of CIP markedly enhanced the heat resistance and wet-heat stability of SM adhesives through physical barrier effects, while optimizing magnetic attraction efficiency. In contrast, Fe_3O_4 nanoparticles achieved rapid magnetic response at low additive levels due to their high saturation magnetization, though nano-aggregation caused a sharp viscosity increase. Scenario-based validation confirmed that CIP-modified adhesives exhibit excellent structural stability in hot and humid kitchen environments, and they could withstand steam exposure, and retain magnetic adsorption properties.

DOI: 10.15376/biores.21.1.873-889

Keywords: SM adhesive; CIP; Fe_3O_4 nanoparticles; Multifunctionality; Bioadhesive

*Contact information: College of Furnishings and Industrial Design, Nanjing Forestry University Nanjing, Jiangsu, China; *Corresponding author: xuwei@njfu.edu.cn*

INTRODUCTION

Adhesives play a pivotal role in various industries, ranging from construction and automotive to electronics and packaging (Shin *et al.* 2024; Ciardiello *et al.* 2025; García-Moreno *et al.* 2025; Shi *et al.* 2025). Traditional synthetic adhesives, while effective, often raise environmental concerns due to their petroleum-based origins and non-biodegradable nature. In recent years, there has been a growing interest in developing sustainable, eco-friendly adhesives derived from renewable resources (Bai *et al.* 2024; Fan *et al.* 2024; Yang *et al.* 2025). Among these, soy-based adhesives have emerged as a promising alternative due to their biodegradability, low cost, and abundant availability (Chen *et al.* 2024; Hou *et al.* 2025). Soy proteins, particularly those derived from defatted soy flour, have been extensively studied for their adhesive properties (Zhang *et al.* 2024).

However, the inherent limitations of soy-based adhesives, such as relatively low water resistance and mechanical strength, have prompted researchers to explore various modification strategies to enhance their performance (Bai *et al.* 2024). One such strategy involves the incorporation of polyamidoamine-epichlorohydrin (PAE) resin, a widely used cross-linking agent that can significantly improve the water resistance and bond strength

of soy-based adhesives (Chang *et al.* 2024; Kan *et al.* 2024). The curing mechanism involves water evaporation and chemical cross-linking between PAE and soybean protein. Under heating conditions, the PAE resin reacts with amino and hydroxyl groups in soy protein to form a covalently cross-linked network, thereby enhancing the adhesive's durability and mechanical properties (Mi *et al.* 2023; Kan *et al.* 2025; Grossi *et al.* 2025). Additionally, the combination of high-temperature and low-temperature defatted soy flour has been shown to optimize the adhesive properties by balancing the protein denaturation and functional group availability (Zheng *et al.* 2017; Yan *et al.* 2022).

In recent years, the development of multifunctional adhesives has emerged as a cutting-edge frontier in materials science, driven by demands for smart and responsive materials in advanced applications (Hu *et al.* 2024; Cao *et al.* 2025; Lima *et al.* 2025). Among these, magnetic adhesives have garnered significant attention due to their unique ability to interact with external magnetic fields, enabling innovative functionalities such as reversible adhesion, electromagnetic shielding, and smart assembly systems (Verna *et al.* 2013; Wang *et al.* 2022; Sha *et al.* 2023). For instance, magnetic adhesive-enabled substrates could serve as reconfigurable mounting platforms for small objects (*e.g.*, children's toys, office supplies, or kitchen utensils), combining structural bonding with on-demand magnetic attachment. To realize such dual functionality, a systematic investigation into the individual effects of magnetic fillers—specifically carbonyl iron powder (CIP) and Fe_3O_4 nanoparticles—within bio-based adhesive matrices is critical. It is worth noting that kitchen environments have stringent requirements for adhesives compared to office and children's daily activity spaces, including exposure to fumes (70 °C), steam (100 °C) and humidity fluctuations (48 to 56% RH) (Xu et al. 2023; Xin et al. 2024).While epoxy resin-based magnetic adhesives incorporating carbonyl iron powder (CIP) exhibit thermal decomposition starting at 375 °C , their petroleum-derived nature and excessive thermal tolerance mismatch practical kitchen demands. This highlights the need for bio-based alternatives that balance functional performance with sustainability (You 2013).

To realize such dual functionality in eco-friendly systems, a systematic investigation into the individual effects of magnetic fillers—specifically CIP and Fe_3O_4 nanoparticles—within bio-based adhesive matrices is critical. In this study, micro-scale CIP (5 μm) and nano-scale Fe_3O_4 (20 nm) are introduced as independent control groups. CIP, which is characterized by high magnetic permeability and low coercivity, was selected due to its ability to provide robust bulk magnetization (Zhang *et al.* 2023; Peng *et al.* 2025). Fe_3O_4 nanoparticles exhibit superparamagnetic behavior and a high specific surface area, while the Fe^{3+} ions on their surface can enhance the bonding performance of PAE-modified soy-based adhesives by forming coordination bonds with amino and hydroxyl groups in the cross-linking network (Mi *et al.* 2023). To suppress aggregation, CIP and Fe_3O_4 were modified with KH-550 (γ-aminopropyl triethoxysilane) and polyacrylic acid (PAA), respectively, ensuring uniform dispersion while strengthening interfacial adhesion (Zhang 2005; You 2013; Song *et al.* 2022). This surface engineering not only ensures homogeneous dispersion, but also thermal degradation of PAA-modified Fe_3O_4 up to a temperature of 150 to 200 °C (Wang *et al.* 2024). Through decoupling the magnetic and mechanical impacts of these fillers, the present work establishes a foundational framework for designing hybrid bio-adhesives tailored to multifunctional kitchen applications.

This study systematically investigates the effects of micro-scale carbonyl iron powder (CIP) and nano-scale Fe_3O_4 nanoparticles on the bonding strength, water resistance, thermal stability, and magnetic responsiveness of SM adhesives, aiming to address the functional demands of bio-based adhesives in high-humidity and high-

temperature kitchen environments (*e.g.*, steam-exposed cutting boards and magnetic storage racks). Through incorporating CIP and Fe_3O_4, Fourier-transform infrared (FTIR) spectroscopy was employed to better understand filler-matrix interfacial interactions, elucidating the synergistic mechanisms between magnetic functionality and adhesive performance. This study focused on developing an adhesive that combines moisture and heat resistance with magnetic adsorption properties. Used as a bonding agent between wood veneers, it enables the production of magnetically adsorbent plywood. This facilitates the creation of magnetic furniture with customizable layouts and stable fixation, such as magnetic knife racks and removable storage modules for kitchen magnetic storage systems. Through the synergistic optimization of interface engineering and particle size effects, this work provides theoretical insights for designing bio-based adhesives tailored to complex humid/thermal environments, facilitating the transition of green materials from laboratory research to practical applications.

EXPERIMENTAL

Materials

The low-temperature defatted soybean meal (LSM) (protein content: 51.4%) and high-temperature defatted soybean meal (HSM) (protein content: 48.7%) were purchased from Anyang Wanhui Bio-technology Co. The PAE resin had a solids content of 13.33%, a pH of 3.98, and a viscosity of 84 mPa·s. It was supplied by Zhejiang Shenghua Yunfeng Holding Group Co., Ltd. Carbonyl iron powder was purchased from Guangzhou Metal Metallurgy Group Co., Ltd., with a particle size of 5 μm. The silane coupling agent KH550 was purchased from Kangjin New Material Technology Co. Tri-iron tetraoxide nanoparticles were purchased from Aladdin Holding Group with a particle size of 20 nm, and PAA was purchased from Shandong Linyi Bangpu Import and Export Co. Eucalyptus veneer (300 mm × 300 mm × 3 mm, moisture content 12% to 14%) was provided by Zhejiang Shenghua Yunfeng Holding Group Co.

Preparation of Magnetic Adhesive

Pretreatment of magnetic fillers

A total of 100 g of carbonyl iron powder pretreatment was weighed, it was configured in 250 mL KH-550 solution (the volume ratio of anhydrous ethanol to distilled water in the solvent is 10:1), and the amount of KH-550 in the added solution was 3% of the mass of carbonyl iron, respectively. The carbonyl iron powder was put into the mixture, and then the mixed solution was ultrasonically dispersed in a water bath at 40 °C with mechanical stirring for 30 min. The mixture was then left to stand for 24 h after completion, so that the KH-550 and the carbonyl iron powder particles could fully react. Finally, the system was placed in a drying oven at 80 °C, dried, and sealed for spare parts (You 2013).

A total of 100 g of Fe_3O_4 nanoparticles was weighed, 10 g of PAA was added to it, and then it was poured into the appropriate amount of demineralized water, next ultrasonic dispersion by ultrasonic cleaner was performed for 10 min, and finally the system was put into the drying box at 60 °C, dried and sealed for spare material preparation (Song *et al.* 2002; Zhang 2005).

Adhesive preparation

The LSM and HSM were blended at a 2:3 mass ratio to prepare composite SM. The PAE resin was diluted to 7% solid content with deionized water. The SM, PAE solution, and magnetic fillers (CIP/Fe_3O_4) were mixed in varying mass ratios under mechanical stirring for 5 min. The formulas are shown in Table 1.

Table 1. Various Adhesive Formulations

Sample	Adhesive Formula				
	SM (g)	Water (g)	PAE (g)	CIP (g)	Fe_3O_4 (g)
SM adhesive	20	39	31	0	-
SM-CIP-15 adhesive	20	39	31	15	-
SM-CIP-25 adhesive	20	39	31	25	-
SM-CIP-35 adhesive	20	39	31	35	-
SM-CIP-45 adhesive	20	39	31	45	-
SM-CIP-55 adhesive	20	39	31	55	-
SM-CIP-65 adhesive	20	39	31	65	-
SM-Fe_3O_4-15 adhesive	20	39	31	-	15
SM-Fe_3O_4-25 adhesive	20	39	31	-	25
SM-Fe_3O_4-35 adhesive	20	39	31	-	35

Preparation of Three-ply Plywood

The SM adhesive was uniformly applied to both sides of the eucalyptus core veneer at a spread rate of 260 g/m². The assembly (core veneer with adhesive and two unglued face veneers) was aligned along the wood grain direction, pre-pressed at 1.3 MPa for 40 min, then hot-pressed at 120 °C and 1.2 MPa for 20 min to fabricate three-ply plywood.

Determination of Adhesive Viscosity

The viscosity of the adhesive was measured using NDJ-1 viscometer (Zhejiang, China). Sampling was according to the Chinese national standard GB/T 2794 (2022). Provisions of the sampling involved stirred to ensure the representativeness of the sample. The number of units to be taken was basically kept the same; in each case, a sufficient amount was collected to accommodate three tests. Additional mixture was retained, as needed, for additional testing.

Water Resistance Test

Plywood water resistance was evaluated according to GB/T 2794 (2022). After conditioning at room temperature for ≥ 24 h, 12 specimens (2.5 cm × 10 cm) were cut from each panel.

Dry strength was tested directly using a UTM 6000 universal testing machine (Shenzhen, China).

Category II wet strength: Specimens were immersed in 63 ± 3 °C water for 3 h, cooled for 10 min, then tested.

Category I wet strength: Specimens were boiled for 4 h, dried at 63 ± 3 °C for 20 h, re-boiled for 4 h, cooled in room-temperature water, then tested.

Fourier Transform Infrared Spectroscopy (FTIR)

The prepared adhesives were cured in an oven at 120 °C and ground into powder. The cured magnetic adhesive powder was tested by KBr pressing method using a VERTEX

80V FTIR spectrometer (Bruker, Germany) with a scanning wave number of 4000 to 400 cm^{-1}, resolution of 4 cm^{-1} and 32 scans.

Thermal Performance Test

Thermal stability was evaluated using a TGA 209F3 thermogravimetric analyzer (NETZSCH, Germany). Samples for TGA analysis were prepared from the adhesives that had been cured in an oven at 120 °C and ground into powder. Subsequently, portions weighing 0.0050 to 0.0100 g were loaded into TGA aluminum pans and heated from 25 to 650 °C at a rate of 20 °C/min under a nitrogen atmosphere with a flow rate of 40.0 mL/min. The relationship of the change of the system quality (w%) was obtained at each temperature (T).

Magnetic Absorption Test

Square plywood specimens (20 mm × 20 mm, n = 10 per group) were cut and deburred. Standardized neodymium iron boron (NdFeB) magnets (20 mm × 10 mm × 2 mm) were vertically contacted with the specimen surface on a non-magnetic platform. As shown in Fig. 1, the plywood specimen was placed flat on a non-magnetic platform. The test commenced with a single magnet being vertically brought into contact with the sample surface and then gently released. If adhesion was maintained, magnets were added incrementally until the maximum number that could be stably held was identified.

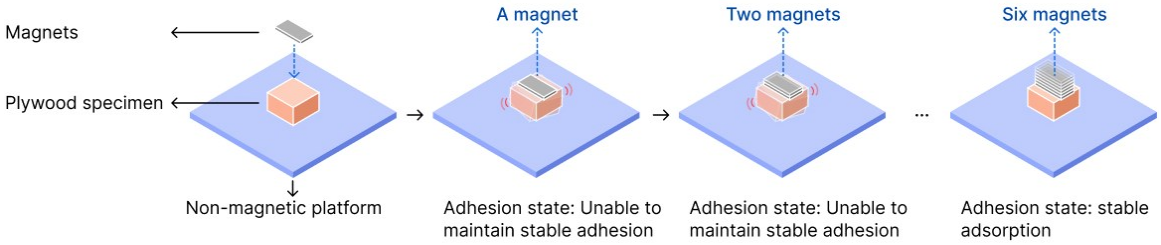

Fig. 1. Magnetic adsorption test diagram

RESULTS AND DISCUSSION

Flow and Viscosity Analysis of Fresh Adhesives

Proper fluidity is a prerequisite for the adhesive to be able to wet and penetrate the veneer surface and finally form mechanical interlocks to achieve bonding. As shown in Fig. 2, increasing Fe_3O_4 loading markedly raised adhesive viscosity and reduced fluidity; for CIP, there was no marked change in the fluidity. The surface of CIP was treated with a coupling agent, and because of its large particle size and low specific surface area, it was uniformly dispersed in the substrate, and it had good interfacial compatibility with the PAE resin-defatted soybean meal matrix. Therefore, it was able to maintain proper adhesion even if the addition amount was increased to 65 g, which is a prerequisite for wetting and penetrating the veneer surface. Even at that addition level, it still maintained suitable fluidity without marked changes. In contrast, although Fe_3O_4 nanoparticles were also modified with coupling agents, their nanoscale size, magnetic interactions, and high specific surface area resulted in particles that were prone to agglomeration (Zhang *et al.* 2021), and the formation of the network structure markedly increased the viscosity of the

system and decreased the fluidity markedly, especially when the amount of the additive was more than 25 g.

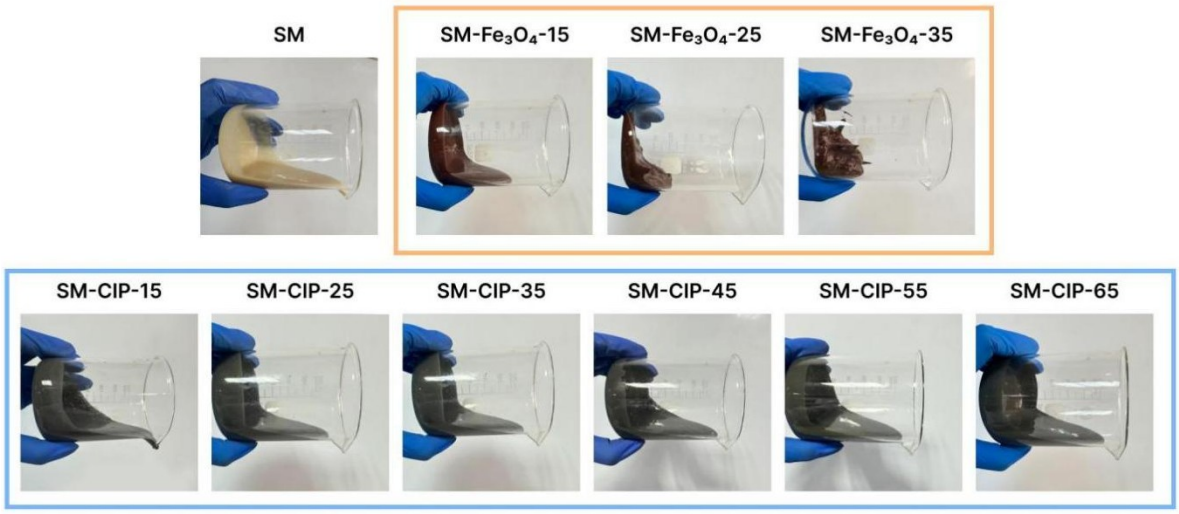

Fig. 2. Adhesive fluidity

Tables 2 and 3 show the effects of CIP and Fe_3O_4 loadings on adhesive viscosity and solids content. As far as the applicability of adhesive technology is concerned, the viscosity range of adhesives used for wood lamination should be between 5,000 and 25,000 mPa·s (Zhang *et al.* 2021; Xu *et al.* 2022). The viscosity of the SM-CIP system increased with CIP addition from 11,909 to 47,550 mPa·s, and it still remained in the wood-laminating adhesives in the ≤ 45 g addition. The uniform dispersion of micron-sized particles and surface hydrophobicity modification effectively slowed down the sharp increase in viscosity; the solid content was linearly increased from 23.4% to 68.0%, indicating that the high loading capacity of the CIP was compatible with the substrate. Thus, the recommended dosage is 35 to 45 g. The viscosity of SM-Fe_3O_4 system soared from 11,900 to 72,600 mPa·s with nanoparticle loadings approaching the upper limit of the process only at loading ≤ 15 g. Nanoclusters markedly degraded the fluidity at high loadings; the increase in solids content was slower, and a maximum loading of ≤ 15 g is recommended to avoid processing failures. The micrometer size of CIP balanced viscosity and functionality through physical filling and interfacial bonding, while the nano-effect of Fe_3O_4 limited its window of applicability due to the tendency of agglomeration.

Table 2. Viscosity and Solid Content of the SM-CIP Adhesive

	CIP Content in SM-CIP Adhesive (g)						
	0	15	25	35	45	55	65
Viscosity(mPa·s)	11909	10786	18483	21315	24652	35138	47550
Solid content (%)	23.39	33.63	40.67	49.67	56.78	60.34	67.96

Table 3. Viscosity and Solid Content of the SM-Fe_3O_4 Adhesive

	Fe_3O_4 Content in SM-Fe_3O_4 Adhesive (g)			
	0	15	25	35
Viscosity(mPa·s)	11909	21356	45632	72568
Solid content (%)	23.39	36.27	41.35	46.01

Water Resistance Analysis of Adhesives

Figure 3A and B show the results of tensile shear strength tests of plywood prepared with different adhesives under dry state and hygrothermal conditions. For the SM-CIP adhesive (Fig. 3A), the dry strength initially increased with CIP loading, peaking at 1.86 MPa (45 g), then declined to 1.20 MPa. This suggests that the moderate dispersion of micrometer-sized CIP markedly enhanced the cross-linking density through the hydrophobic modification of the surface and the interfacial bonding, whereas the aggregation of particles at the high content led to the disruption of the continuity of the matrix. The category I wet strength decreased continuously from 0.88 to 0.50 MPa with the increase of CIP addition from 15 to 65 g, while the category II wet strength maintained a high level in the range of 25 to 45 g, indicating that the surface modification of CIP effectively suppressed the penetration of water molecules in the moderate addition. However, the interfacial defects were aggravated in the high content. Even at the high addition level of 55 g, the category II wet strength remained at 1.08 MPa (87.1% retention of dry strength), highlighting the robustness of its water resistance performance (Sadare *et al.* 2020).

In contrast, the dry state strength of SM-Fe_3O_4 adhesive (Fig. 3B) reached 1.65 MPa at 25 g (22.2% enhancement over the base SM), but plummeted to 1.09 MPa at 35 g, reflecting the negative effect of the agglomeration effect of the nanoparticles on the integrity of the adhesive layer. The water resistance showed marked differences: the category I wet strength decreased sharply with increasing addition (1.00→0.63 MPa, a 37% decrease), while the category II wet strength rose to 1.41 MPa at 25 g (up to 85.5% of the dry strength), but excessive addition still led to performance collapse (Zeng *et al.* 2022; Chen *et al.* 2023).

The lower category I wet tensile shear strength indicated limited resistance to prolonged boiling, suggesting that the current SM-based adhesives are suitable for interior applications.

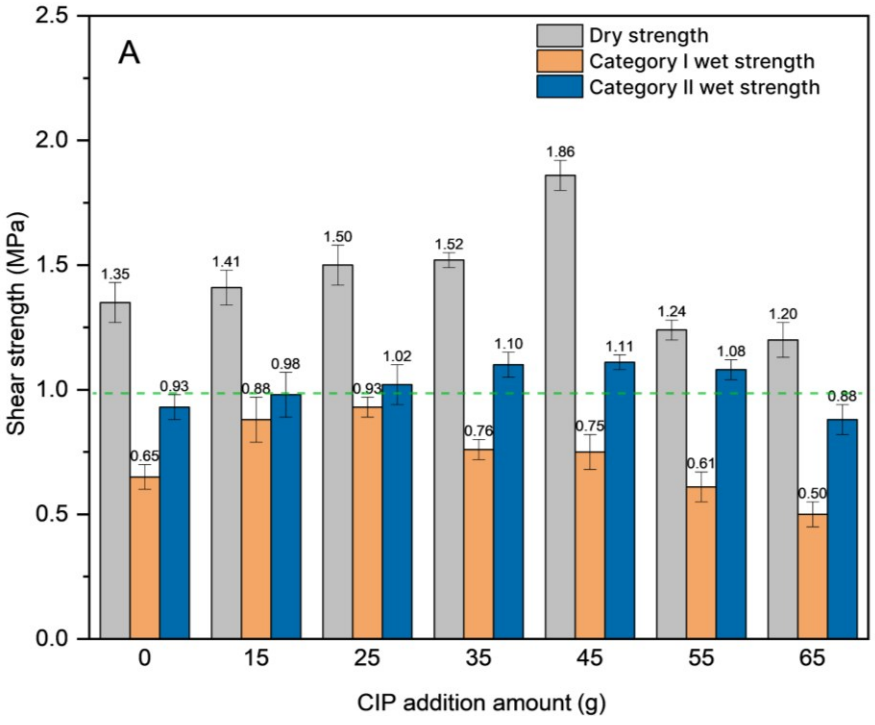

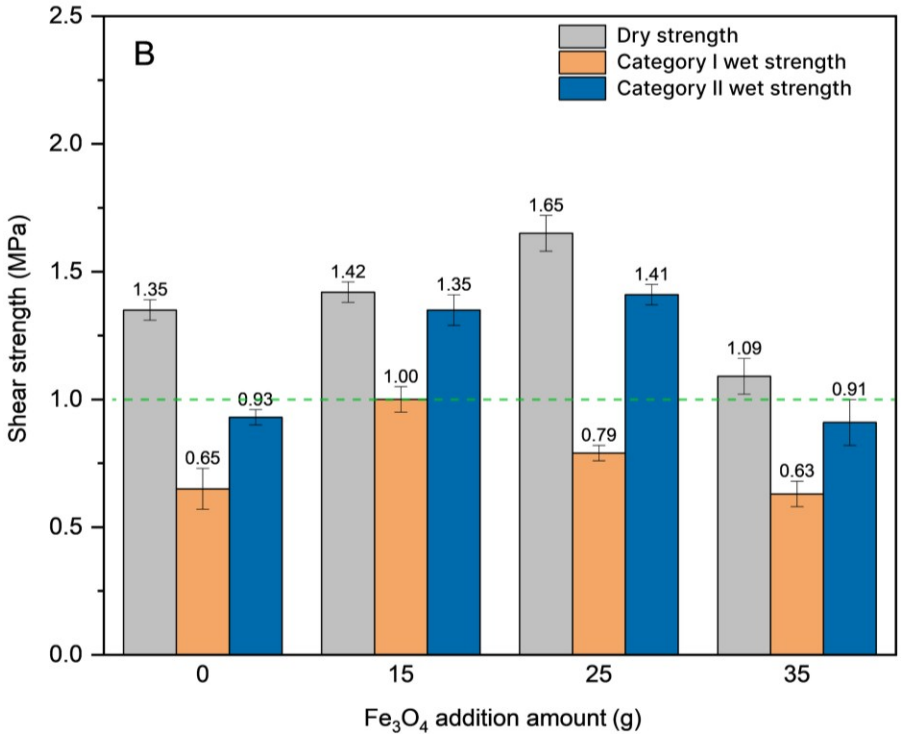

Fig. 3. Gluing strength of different adhesives: (A) gluing strength of SM-CIP adhesive; (B) gluing strength of SM-Fe_3O_4 adhesive

Visual Appearance of Cured Adhesives

The prepared adhesives were cured in an oven at 120 °C. The base SM adhesive showed marked cracks (maximum crack density) in the adhesive layer due to the low solid content and moisture evaporation during curing, which was directly related to the pore structure due to the lack of hydrophobic components (Li *et al.* 2022). The introduction of functional particles markedly improved this defect. Figure 4 shows that crack density in the SM-Fe3O4 system decreased progressively from severe (15 g) to negligible (35 g).

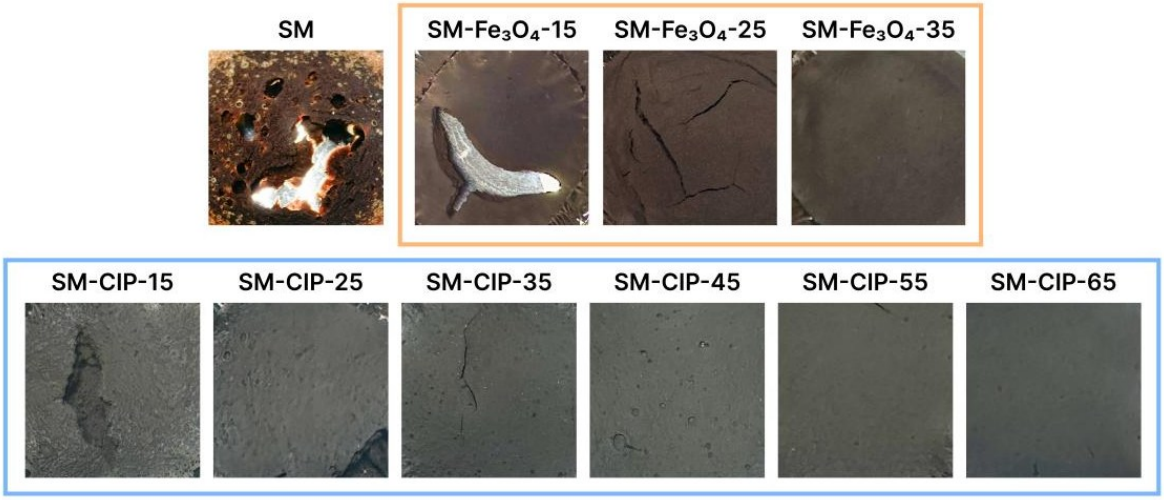

Fig. 4. Visual appearance of different cured adhesives

In contrast, the SM-CIP system achieved a completely crack-free adhesive layer at 45 to 65 g of loadings, and only microcracks are present at 25 to 35 g. The optimization effect was marked. For trace cracks, the optimization effect was markedly better than that of the Fe_3O_4 system.

FTIR Analysis

Infrared spectra of Fig. 5A (SM-CIP adhesive) and Fig. 5B (SM-Fe_3O_4 adhesive) reveal the differential effect of additives on the chemical structure of the adhesive. The FTIR spectra of SM-CIP adhesive were analyzed in the range of 3427 cm^{-1} (O-H/N-H stretching vibrations), 2927 cm^{-1} (-CH symmetry vibration), 1641 cm^{-1} (amide I, C=O stretching vibration), 1532 cm^{-1} (amide II, N-H bending/C-N stretching, and 1046 cm^{-1} (C-O/C-N stretching vibration) and showed characteristic peaks, in which the vibration amplitudes at 1641 cm^{-1}, 1532 cm^{-1}, and 1046 cm^{-1} were markedly enhanced with the increase of CIP addition (Rad *et al.* 2015; Zhang *et al.* 2021; Li *et al.* 2022; Chen *et al.* 2023).

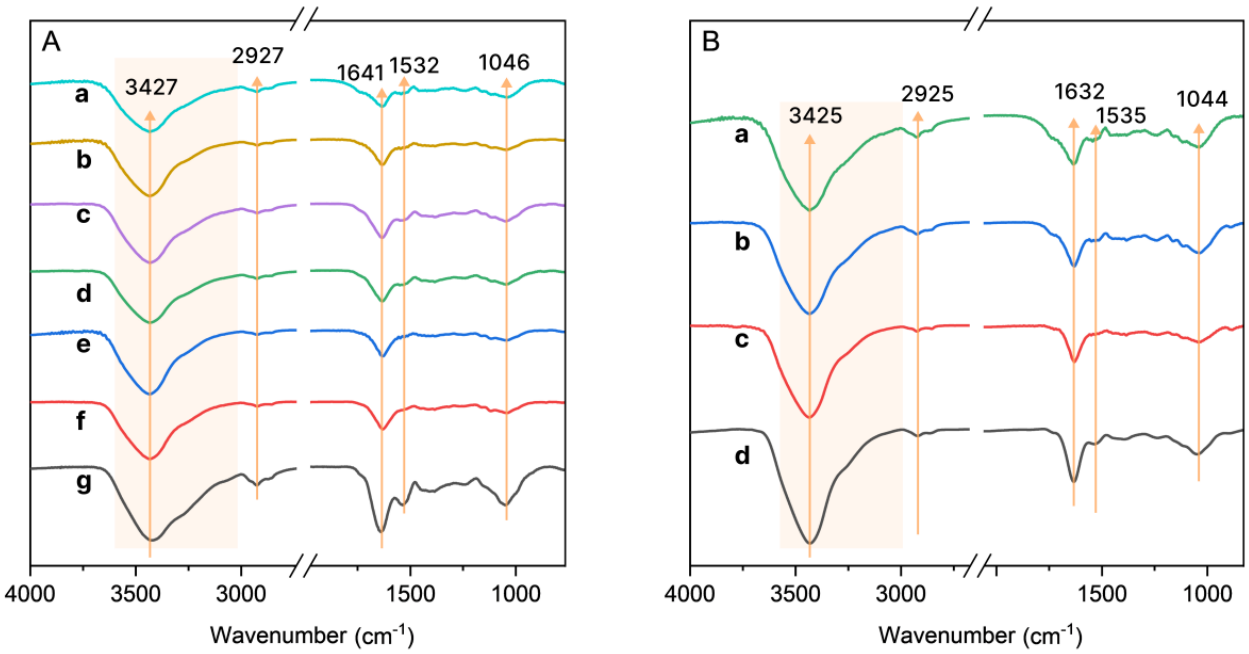

Fig. 5. FTIR spectra of different adhesive samples: A: a (SM), b (SM-CIP-15), c (SM-CIP-25), d (SM-CIP-35), e (SM-CIP-45), f (SM-CIP-55), g (SM-CIP-65); B: a (SM), b (SM-Fe_3O_4-15), c (SM-Fe_3O_4-25), d (SM-Fe_3O_4-35)

The chemical reaction between PAE and SM crosslinking is shown in Fig. 6. This suggests that the micron-sized particles of CIP promoted the cross-linking reaction between PAE resin and soybean flour matrix through surface modification, which strengthened the hydrogen bonding network and interfacial chemical bonding of the amide structure, and thus enhances the cross-linking density and structural stability. In contrast, the vibrational amplitude of SM-Fe_3O_4 adhesive at 1632 cm^{-1} (amide I) increased with the increase of Fe_3O_4 content, but the peak position was shifted lower than that of SM-CIP (shifted from 1641 to 1632 cm^{-1}), and nanoparticles may have interfered with the electronic conjugation of C=O.

The continuous enhancement of SM-CIP at 1046 cm^{-1} and the synergistic optimization of the amide structure (1532 cm^{-1} amplitude enhancement) together support its excellent water resistance, whereas the shift of the amide I peak position and vibration amplitude of SM-Fe_3O_4 variations reflect the coexistence of interfacial cross-linking enhancement and structural defects brought about by the nano-effect. It is noted that directly quantifying new amide bonds from curing is complicated by the inherent amide signals from the soy protein.

The observed spectral changes are therefore attributed to the restricted molecular mobility and altered chemical environment resulting from a more densely cross-linked network formed between PAE and the soy protein matrix. This interpretation is consistent with the improved mechanical and water-resistant properties. In summary, the micron-scale dispersion of CIP effectively balanced functionality and structural integrity through surface modification, while the nanoparticle addition of Fe_3O_4 needs to further optimize the dispersion process to inhibit agglomeration and strengthen chemical bonding.

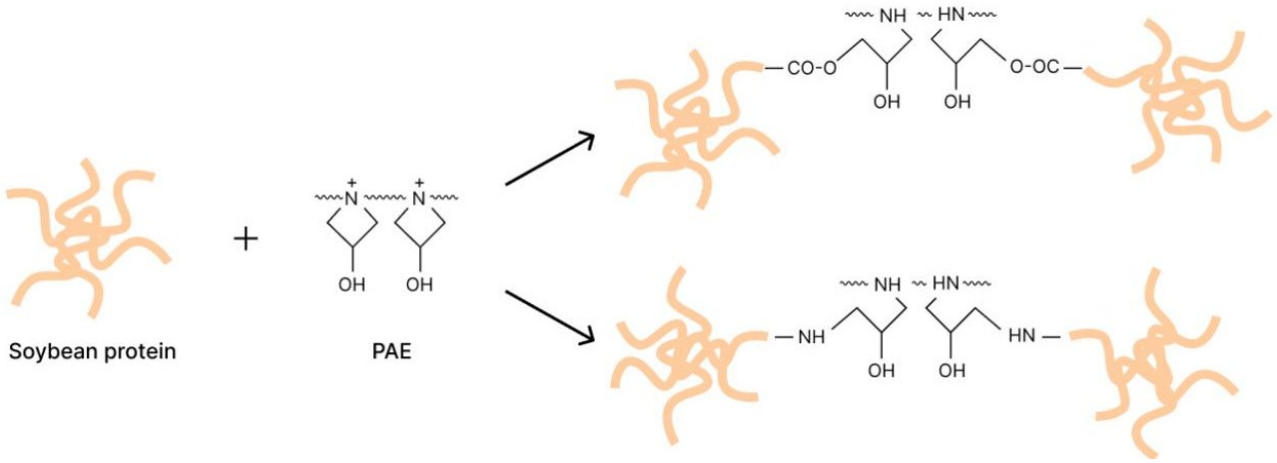

Fig. 6. Chemical reaction of PAE crosslinking with SM

Analysis of Thermal Properties of Adhesives

The thermal degradation process of SM adhesives is characterized by three stages: the first stage (room temperature ~210 °C) is mainly the escape of adsorbed and bound water; the second stage (210 to 250 °C) involves the thermal degradation of unstable soybean polysaccharide side chains and small molecules (oligosaccharides, free amino acids); and the third stage (250 to 600 °C) corresponds to the deeper decomposition of the protein skeleton structure and the crosslinked network of PAE resin (Chen *et al.* 2023; Li *et al.* 2023; Shan *et al.* 2024).

As shown in Fig. 7, the thermal behaviors were markedly altered after the introduction of CIP or Fe_3O_4: the initial decomposition temperatures of both SM-CIP and SM-Fe_3O_4 adhesives were greater than 150 °C, and the physical barrier formed by CIP through the micrometer-scale dispersion (degradation peak at 310 °C) slowed down the second-stage volatile fraction release. It also promoted the third-stage dense char layer formation (82.8% char residue), while Fe_3O_4 nanoparticles accelerated the second stage pyrolysis reaction (degradation peak temperature down to 299 °C) through high specific surface area and catalytic activity and achieved 67.8% char residue. This formulation was able to maintain interfacial stability over time in a high-temperature steam environment in a kitchen (typical temperature ≈100 °C).

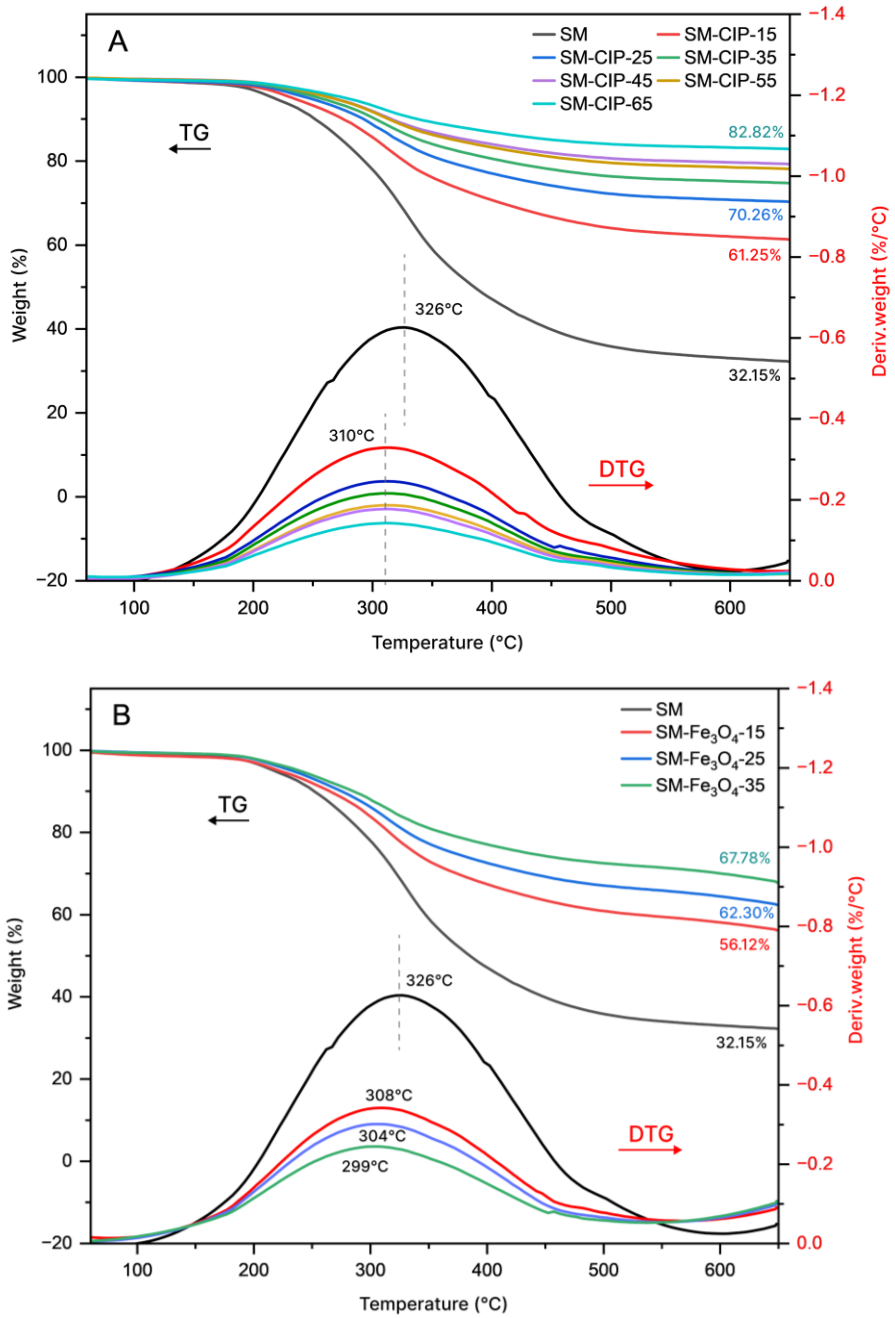

Fig. 7. A: TG and DTG analyses of the SM-CIP adhesive; B: TG and DTG analyses of the SM-Fe_3O_4 adhesive

Analysis of Magnetic Attraction of Adhesives

Figure 8 shows the test method for magnetic adhesion. Table 4 lists the number of magnets required to achieve complete adsorption of wood blocks at different additive levels for SM-CIP and SM-Fe_3O_4 adhesives. The SM-CIP adhesive achieved stable magnetic attraction at high additive levels of 45 to 65 g through micron-scale physical filling and interfacial bonding (only 4 to 5 magnets), while SM-Fe_3O_4 adhesive achieved equivalent magnetic response (5 to 6 magnets) at a low additive level of 25 to 35 g by virtue of high saturation magnetization of nanoparticles and surface modification-enhanced

interactions. For humidity resistance, modified SM-CIP (45 to 55 g) enabled humidity- and heat-resistant magnetic carriers in kitchens (60.34% solid content and 5-magnet shedding resistance), taking into account functionality, safety, and environmental adaptability.

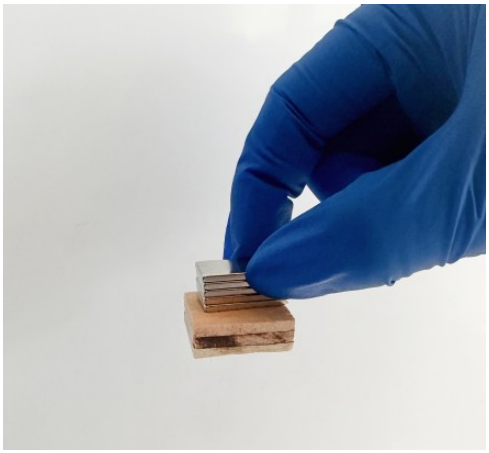

Fig. 8. Test method for magnetic attraction

Table 4. Number of Fully Adsorbed Magnets for Different Adhesives

	CIP Content in SM-CIP Adhesive (g)						Fe_3O_4 Content in SM-Fe_3O_4 Adhesive (g)		
	15	25	35	45	55	65	15	25	35
Number of magnets	7	6	6	5	5	4	7	6	5

CONCLUSIONS

1. In this study, the differences in the properties of carbonyl iron powder (CIP) and nanoscale Fe_3O_4-modified soybean meal (SM) adhesives were systematically investigated to reveal the mechanisms of particle size effects and interfacial interactions on the comprehensive performance of the adhesives. The results showed that the micron-scale dispersion characteristics of CIP endowed the SM-CIP system with excellent flowability (21,500 to 24,700 mPa·s at viscosities ≤ 45 g) and high char residue (82.8%). Its hydrophobic interfacial design effectively inhibited interfacial peeling under hot and wet environments (87.1% retention of Category II wet strength); whereas the Fe_3O_4's nanoscale highly saturated magnetization property enabled the SM-Fe_3O_4 system to reach the viscosity standard (21,400 mPa·s) at a low addition level (≤ 15 g) and achieve a sensitive magnetic response (5 to 6 magnets are required at 25 to 35 g), but they were limited by a sudden increase in viscosity due to nano-agglomeration (up to 72,600 mPa·s at 35 g) with a degradation of hygroscopic strength (37% decrease in Category I wet strength).
2. Scenario-based analysis showed that the moisture-resistant SM-CIP (60.3% solids) met the hygrothermal stability needs of the kitchen scenario. The developed adhesive successfully served dual functions: as a structural binder for wood veneers in plywood manufacturing, and as a magnetic component enabling the resulting composite to function in magnetic storage applications. Combined with the filler-substrate interfacial bonding mechanism resolved by Fourier transform infrared (FTIR) spectrometry, this

study provides a theoretical basis and technical paradigm for the multifunctionalized design and precise scenario-adaptation of biobased adhesives and promotes the expansion of the application of green adhesives in the fields of intelligent manufacturing and sustainable materials. The adhesives demonstrated potential for interior applications such as kitchen magnetic storage systems, though further optimization is needed for high-humidity exterior conditions. Meanwhile, the long-term stability and anti-settling properties of the fresh adhesive will be evaluated in subsequent studies.

REFERENCES CITED

Bai, M., Chen, S., Li, X., Aladejana, J. T., Li, C., Cao, J., and Li, J. (2024). "Development of soybean meal-based adhesive with multiple functions *via* a dual cross-linked tailoring-making strategy," *Polymer* 300, article 126972. https://doi.org/10.1016/j.polymer.2024.126972

Bai, Y., Wan, J., Zhang, X., Huo, H., Shi, H., Yang, H., Yang, Y., Ran, X., and Yang, L. (2024). "Bonding wood *via* an organic-inorganic hybrid adhesive with excellent mechanical and fire resistance properties," *Construction and Building Materials* 457, article 139495. https://doi.org/10.1016/j.conbuildmat.2024.139495

Cao, F., Xu, Y., Hua, X., Wang, Q., Qiao, Z., and Fang, Z. (2025). "Preparation of a multifunctional soybean protein isolate-based adhesive with enhanced mechanical and flame retardancy properties *via* the synergistic effect between phosphorylated chitosan and quaternary ammonium-functionalized MXene," *International Journal of Biological Macromolecules* 296, article 139684. https://doi.org/10.1016/j.ijbiomac.2025.139684

Chang, J., Kan, Y., Han, S., Wei, S., and Gao, Z. (2024). "Effects of dehydration time on performances of polyamidoamine-epichlorohydrin resin and its modified soybean-based adhesive," *International Journal of Adhesion and Adhesives* 134, 103813. https://doi.org/10.1016/j.ijadhadh.2024.103813

Chen, H., Jiang, K., Wu, Q., Zhang, X., Qian, C., and Fan, D. (2024). "Mussel byssus cuticle-inspired low-carbon footprint soybean meal adhesives with high-strength and anti-mildew performance," *Industrial Crops and Products* 222, article 119433. https://doi.org/10.1016/j.indcrop.2024.119433

Chen, S., Fan, D., and Gui, C. (2023). "Investigation of humidity-heat aging resistance of a soy protein adhesive fabricated by soybean meal and lignin-based polymer," *Polymer Testing* 120, article 107971. https://doi.org/10.1016/j.polymertesting.2023.107971

Chen, S., Li, X., Bai, M., Shi, S. Q., Aladejana, J. T., Cao, J., and Li, J. (2023). "Oyster-inspired carbon dots-functionalized silica and dialdehyde chitosan to fabricate a soy protein adhesive with high strength, mildew resistance, and long-term water resistance," *Carbohydrate Polymers* 319, article 121093. https://doi.org/10.1016/j.carbpol.2023.121093

Ciardiello, R., Belingardi, G., Martorana, B., Brunella, V., Hodge, S. A., Galhena, D. T. L., Lin, Y., and Ferrari, A. C. (2025). "Reversible graphene-based adhesives for automotive applications," *International Journal of Adhesion and Adhesives* 138, 103935. https://doi.org/10.1016/j.ijadhadh.2025.103935

Fan, R., Li, H., Aladejana, J. T., Li, K., Zeng, G., Dong, Y., Tian, D., Yao, Z., Gui, C., and Li, J. (2024). "Soybean protein 'mechanically interlocked' bonding of polysaccharide and MXene to improve the strength and toughness of biomass adhesive," *Industrial Crops and Products* 221, article 119429. https://doi.org/10.1016/j.indcrop.2024.119429

García-Moreno, M., Alía, C., Domínguez, C., Garijo, L., and Gómez, F. (2025). "Study of electrical conductivity in epoxy-based adhesives and polyurethane adhesives through the addition of graphene nanoplatelets before and after thermal aging," *International Journal of Adhesion and Adhesives* 139, article 103973. https://doi.org/10.1016/j.ijadhadh.2025.103973

GB/T 2794 (2022). "Determination for viscosity of adhesives," Standardization Administration of China, Beijing, China.

Grossi, B., Pizzo, B., Siano, F., Varriale, A., and Mabilia, R. (2025). "Formaldehyde-free wood adhesives based on protein materials from various plant species," *Results in Engineering* 25, article 104033. https://doi.org/10.1016/j.rineng.2025.104033

Hou, M., Zhang, Q., Lei, H., Zhou, X., Du, G., Pizzi, A., Essawy, H., and Xi, X. (2025). "Mildew resistant modified starch adhesive by soybean meal flour crosslinking with excellent bonding properties," *Carbohydrate Polymers* 354, article 123247. https://doi.org/10.1016/j.carbpol.2025.123247

Hu, Y., Bao, Z., Li, Z., Wei, R., Yang, G., Qing, Y., Li, X., and Wu, Y. (2024). "Develop a novel and multifunctional soy protein adhesive constructed by rosin acid emulsion and TiO2 organic-inorganic hybrid structure," *International Journal of Biological Macromolecules* 277, article 134177. https://doi.org/10.1016/j.ijbiomac.2024.134177

Kan, Y., Chang, J., Wei, S., Li, J., Gui, C., Han, S., and Gao, Z. (2024). "A synergistic strategy for formulating a facile and cost-effective soybean protein-based adhesive *via* co-crosslinking and inorganic hybridization," *International Journal of Biological Macromolecules* 283, article 137569. https://doi.org/10.1016/j.ijbiomac.2024.137569

Kan, Y., Zheng, Y., Wei, S., Han, S., Li, J., and Gao, Z. (2025). "Ammonium salt-induced soybean flour-based adhesive with stable low viscosity, long open time, excellent water retention and bonding property," *Industrial Crops and Products* 226, article 120724. https://doi.org/10.1016/j.indcrop.2025.120724

Li, X., Zhang, F., Li, J., Xia, C., and Li, J. (2022). "Evaluation performance of soybean meal and peanut meal blends-based wood adhesive," *Polymer Testing* 109, article 107543. https://doi.org/10.1016/j.polymertesting.2022.107543

Li, Z., Yan, Q., Shen, Y., Ma, C., Zhang, S., and Jin, T. (2023). "Thermal-driven cationic waterborne polyurethane crosslinker with oxime-based and catechol structure for the preparation of soybean protein-based adhesive with excellent adhesion properties," *International Journal of Adhesion and Adhesives* 126, article 103475. https://doi.org/10.1016/j.ijadhadh.2023.103475

Lima, R., Costa, P., Nunes-Pereira, J., Silva, A. P., Tubio, C. R., and Lanceros-Mendez, S. (2025). "Additive manufacturing of multifunctional epoxy adhesives with self-sensing piezoresistive and thermoresistive capabilities," *Composites Part B: Engineering* 293, article 112130. https://doi.org/10.1016/j.compositesb.2025.112130

Mi, Y., Chen, B., Kan, Y., Bai, Y., and Gao, Z. (2023). "Effects of wood dyestuff on the bonding properties of soybean-based adhesive for commercial plywood production," *International Journal of Adhesion and Adhesives* 124, article 103389. https://doi.org/10.1016/j.ijadhadh.2023.103389

Peng, J., Wang, D. W., Cheng, Z. Y., Yang, M. F., Liu, J. T., and Wang, M. (2025). "Improving microwave absorption performance of carbonyl iron powder by regulating geometric dimensions and electromagnetic-dielectric synergism," *Composites Part A: Applied Science and Manufacturing* 190, article 108719. https://doi.org/10.1016/j.compositesa.2025.108719

Rad, S. A., Khodaverdiloo, K. R., Karamoddin, M., Varaminian, F., and Peyvandi, K. (2015). "Kinetic study of amino acids inhibition potential of glycine and l-leucine on the ethane hydrate formation," *Journal of Natural Gas Science and Engineering* 26, 819-826. https://doi.org/10.1016/j.jngse.2015.06.053

Sadare, O. O., Daramola, M. O., and Afolabi, A. S. (2020). "Synthesis and performance evaluation of nanocomposite soy protein isolate/carbon nanotube (SPI/CNTs) adhesive for wood applications," *International Journal of Adhesion and Adhesives* 100, article 102605. https://doi.org/10.1016/j.ijadhadh.2020.102605

Sha, Z., Cheng, X., Charles, A. D., Zhou, Y., Islam, M. S., Rider, A. N., Peng, S. H., Lim, M., Timchenko, V., and Wang, C. H. (2023). "*In-situ* aligning magnetic nanoparticles in thermoplastic adhesives for contactless rapid joining of composite structures," *Composite Structures* 321, article 117304. https://doi.org/10.1016/j.compstruct.2023.117304

Shan, J., Yang, C., Liu, G., Cao, L., Wu, J., Zhang, Y., and Yu, W. (2024). "An organic-inorganic dual network built in fast-growing wood veneers to improve the flame retardant and mechanical properties of plywood," *Journal of Building Engineering* 97, article 110886. https://doi.org/10.1016/j.jobe.2024.110886

Shi, J., Li, X., Li, A., Wei, H., Zhang, E., and Zhang, W. (2025). "Polyurethane hot-melt adhesives for strong and tough adhesion," *European Polymer Journal* 228, article 113814. https://doi.org/10.1016/j.eurpolymj.2025.113814

Shin, Y., Qiao, Y., Nickerson, E. K., Trevino, A. A., Gilliam, M., Garner, G., Lukitsch, M., Carlson, B. E., and Simmons, K. L. (2025). "Functional group activation and coupling agent migration induced by plasma treatment in adhesive for enhanced toughness of metal-composite joints," *Progress in Organic Coatings* 200, article 109050. https://doi.org/10.1016/j.porgcoat.2024.109050

Song, X. Z., Zhu, Z. P., Zhou, P., He, M. P., Jiang, Y. K., and Wang, Z. G. (2022) . "Study on the dispersion characteristics and mechanism of Fe3O4 by polyacrylic acid," *Chinese Journal of Corrosion and Protection* 42(03), 479-485. https://doi.org/10.7666/d.Y848550

Verna, E., Cannavaro, I., Brunella, V., Koricho, E. G., Belingardi, G., Roncato, D., Martorana, B., Lambertini, V., Neamtu, V. A., and Ciobanu, R. (2013). "Adhesive joining technologies activated by electro-magnetic external trims," *International Journal of Adhesion and Adhesives* 46, 21-25. https://doi.org/10.1016/j.ijadhadh.2013.05.008

Wang, L., Guo, J. X., Chen, X. W., Li, C., Kiyingi, W., Xiong, R. Y., Zhang, X. J., and Gao, C. H. (2024). "Fe3O4/AM-PAA/Ni nanomagnetic spheres: A breakthrough in *in-situ* catalytic reduction of heavy oil viscosity," *Journal of Analytical and Applied Pyrolysis* 181, article 106664. https://doi.org/10.1016/j.jaap.2024.106664

Wang, T., Zhang, P., Yang, X., Zhang, Y., Zhang, J., He, X., Gu, P., and Zhao, Y. (2022). "Rapidly switchable double-layered adhesive modified by magnetic field," *Chemical Engineering Journal* 438, article 135441. https://doi.org/10.1016/j.cej.2022.135441

Xin, J., Shi, X., Ye, F., Zhenlei, C., Yin, P., and Miao, B. (2024). "Evaluation of the air quality and the thermal comfort in the kitchen fume environment under the fresh air supplement," *Results in Engineering* 23, article 102681. https://doi.org/10.1016/j.rineng.2024.102681

Xu, X., Li, C., Dong, J., Meng, C., and Hu, K. (2023). "Improving kitchen environment comfort and health: A comprehensive evaluation method based on objective and subjective factors," *Energy and Buildings* 301, article 113700. DOI: https://doi.org/10.1016/j.enbuild.2023.113700

Xu, Y., Zhang, X., Liu, Z., Zhang, X., Luo, J., Li, J., Shi, S. Q., Li, J., and Gao, Q. (2022). "Constructing SiO_2 nanohybrid to develop a strong soy protein adhesive with excellent flame-retardant and coating ability," *Chemical Engineering Journal* 446, article 137065. https://doi.org/10.1016/j.cej.2022.137065

Yan, Q., Ma, C., Liang, Z., and Zhang, S. (2022). "High-temperature soybean meal adhesive based on disulfide bond rearrangement and multiple crosslinking: Water resistance and prepressing adhesion," *Journal of Cleaner Production* 373, article 133709. https://doi.org/10.1016/j.jclepro.2022.133709

Yang, Z., Ji, X., Sha, X. L., Ding, J., Cheng, L., and Li, G. (2025). "An eco-friendly adhesive with ultra-strong adhesive performance," *Polymer Chemistry* 16(8), 954-962. https://doi.org/10.1039/d4py01398k

Yao, T., Cui, T., Fang, X., Yu, J., Cui, F., and Wu, J. (2013). "Preparation of yolk/shell Fe3O4@ polypyrrole composites and their applications as catalyst supports," *Chemical Engineering Journal* 225, 230-236. DOI: 10.1016/j.cej.2013.02.026

You, Y. C. (2013). *Development of Magnetic Adhesive*, Master's Thesis, University of Electronic Science and Technology, Sichuan, China.

Zeng, Y. Y., Long, H., Wei, G. Y. and Wu, Q. (2022). "Fe3O4@C Interface modification and drug transport properties of nanoparticles," *Functional Materials* 53(03), 3108-3114. https://doi.org/10.3969/j.issn.1001-9731.2022.03.014

Zhang, X. (2013). *Preparation of Magnetic Microspheres of Polyacrylic Acid and Their Adsorption Properties*, Master's Thesis, Tianjin University, China.

Zhang, H., Wang, L., Li, H., Chi, Y., Zhang, H., Xia, N., Ma, Y., Jiang, L., and Zhang, X. (2021). "Changes in properties of soy protein isolate edible films stored at different temperatures: Studies on water and glycerol migration," *Foods* 10(8), article 1797. https://doi.org/10.3390/foods10081797

Zhang, L., Gao, H., Zhang, P., Jiang, X., Zhao, Y., Yin, L., Zhou, D., Zhang, H. X., Xie, J. L., and Deng, L., *et al.* (2023). "Epoxy resin/2-imidazole coated carbonyl iron powder: Synthesis, structure and corrosion performance," *Materials Chemistry and Physics* 306, article 128035. https://doi.org/10.1016/j.matchemphys.2023.128035

Zhang, Y., Liu, Z., Xu, Y., Li, J., Shi, S. Q., Li, J., and Gao, Q. (2021). "High performance and multifunctional protein-based adhesive produced *via* phenol-amine chemistry and mineral reinforcement strategy inspired by arthropod cuticles," *Chemical Engineering Journal* 426, article 130852. https://doi.org/10.1016/j.cej.2021.130852

Zhang, Z., Bian, Y., Li, Z., Zhang, A., Zhang, Y., Kang, H., and Li, J. (2024). "Smart construction of metal chelating for enhancing waterborne polyurethane multi-crosslinked soybean meal adhesives," *International Journal of Adhesion and Adhesives* 132, article 103725. https://doi.org/10.1016/j.ijadhadh.2024.103725

Zheng, P., Lin, Q., Li, F., Ou, Y., and Chen, N. (2017). "Development and characterization of a defatted soy flour-based bio-adhesive crosslinked by 1, 2, 3, 4-butanetetracarboxylic acid," *International Journal of Adhesion and Adhesives* 78, 148-154. https://doi.org/10.1016/j.ijadhadh.2017.06.016

Article submitted: June 29, 2025; Peer review completed: July 26, 2025; Revised version received: November 7, 2025; Accepted: November 30, 2025; Published: December 10, 2025.
DOI: 10.15376/biores.21.1.873-889